Journal of ELECTRONIC MATERIALS
DOI: 10.1007/s11664-013-2472-8


# Thermoelectric Generators for Automotive Waste Heat Recovery Systems Part II: Parametric Evaluation and Topological Studies

SUMEET KUMAR,[1,3] STEPHEN D. HEISTER,[1] XIANFAN XU,[1] JAMES R. SALVADOR,[2] and GREGORY P. MEISNER[2]

1.—School of Mechanical Engineering, Purdue University, West Lafayette, IN, USA. 2.—General Motors Global R&D, Warren, MI, USA. 3.—e-mail: kumar94@purdue.edu

A comprehensive numerical model has been proposed to model thermoelectric generators (TEGs) for automotive waste heat recovery. Details of the model and results from the analysis of General Motors' prototype TEG were described in part I of the study. In part II of this study, parametric evaluations are considered to assess the influence of heat exchanger, geometry, and thermoelectric module configurations to achieve optimization of the baseline model. The computational tool is also adapted to model other topologies such as transverse and circular configurations (hexagonal and cylindrical) maintaining the same volume as the baseline TEG. Performance analysis of these different topologies and parameters is presented and compared with the baseline design.

**Key words:** Thermoelectric generators, waste heat recovery, automotive exhaust, skutterudites

## INTRODUCTION

In part I of this study, we developed a comprehensive model to analyze the performance of thermoelectric generators (TEGs) based on automotive exhaust gas as the heat source.[1] The model was then employed to assess the electric power generation of General Motors' prototype.[2,3] In the second part of the study, presented here, parametric evaluation of the baseline model is performed with the goal of achieving optimized configurations. Several other topologies are also discussed in detail.

Morelli[4] emphasized that internal finning and diffuser arrangements in the TEG system are important for minimizing the temperature difference between the hot gas and the hot side of the thermoelectric device. Hence, design of an efficient heat exchanger is key to enhance the heat transfer from the poorly conducting exhaust gas to the thermoelectric modules (TEMs) for improved electrical power generation. It is a known fact that the power-generating capacity of TEMs depends on the temperature difference across the junctions. Temperatures across the TEMs are found to drop considerably due to the rapid drop in the exhaust gas temperature as it advances along the length of the TEG. Skutterudites have high $ZT$ at temperatures $>300°C$, hence the TEMs near the rear end of the TEG have low power output as a result of the much smaller temperature gradient across them as compared with modules at the leading edge of the system. On the other hand, TEMs based on bismuth telluride perform much better than skutterudites at lower temperatures ($T < 250°C$). Hence, using a hybrid configuration could help to increase the system's electrical power output for the given thermal profile inside the TEG. In addition to this arrangement, TEMs would perform better if they face the hottest temperatures inside the TEG. This could only be achieved with modifications of the TEG geometry. Crane et al.[5] described the evolution from planar topography of a TEG to a cylindrically shaped TEG during phases 3 and 4 of the BSST-led

(Received September 10, 2012; accepted January 4, 2013)

Published online: 05 March 2013

US Department of Energy (DOE) project. The benchtest of BSST's cylindrical TEG (designed for the Ford Lincoln MKT and the BMW X6) reported electrical power generation exceeding 700 W at the National Renewable Energy Laboratory based in Colorado. The heat gun source was capable of maintaining 700°C at the hot side of the TEGs, while the cold side was kept at 20°C using a high-capacity chiller.

To address these issues, rigorous optimization of TEGs of various shapes is performed in this work, which represents the second part of this two-part study. The tools developed in the first part of this two-part study[1] are utilized to run optimization routines on various parameters to study the dependence of outputs and to optimize the baseline model design. Results from various topologies starting from rectangular to circular shapes with the same volume constraints are discussed too. The dimensions of the TEG topologies are constrained by practical bounds of the vehicle of interest. The next section provides a description of the topologies considered, followed by the results and conclusions from the study.

## STUDY OF TOPOLOGIES

In this section, various topologies analyzed are discussed. As mentioned in the "Introduction," variants of the baseline configuration are studied, referred to as longitudinal configurations. Four different topologies are discussed throughout this work. The topologies are named as rectangular or circular depending upon their cross-sectional geometry.

### Rectangular Topology

The topologies having a rectangular box-like shape are grouped as rectangular topology as shown in Fig. 1. The names of the model—longitudinal and transverse—are derived from the way the TEMs are placed with respect to the exhaust flow direction. The longitudinal model shown in Fig. 1a, b was discussed in part I of this two-part study.[1] GM's prototype design is termed as the baseline model, being a longitudinal model variant. The transverse model, as shown in Fig. 1c, d, is proposed as an alternative configuration to the traditional, longitudinal

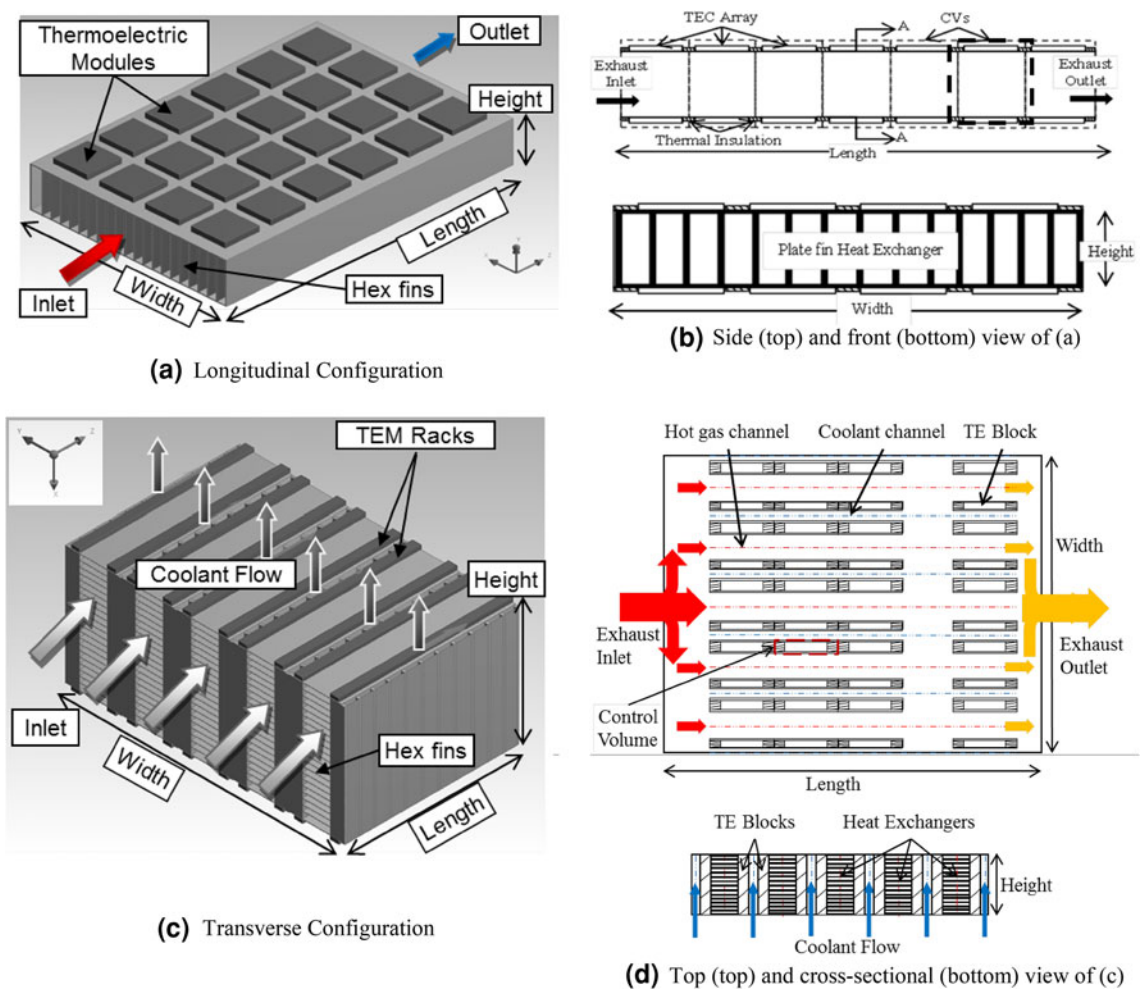


Fig. 1. Rectangular topologies, showing the arrangement of thermoelectric modules, heat exchanger placement, and exhaust flow direction through the thermoelectric generators.

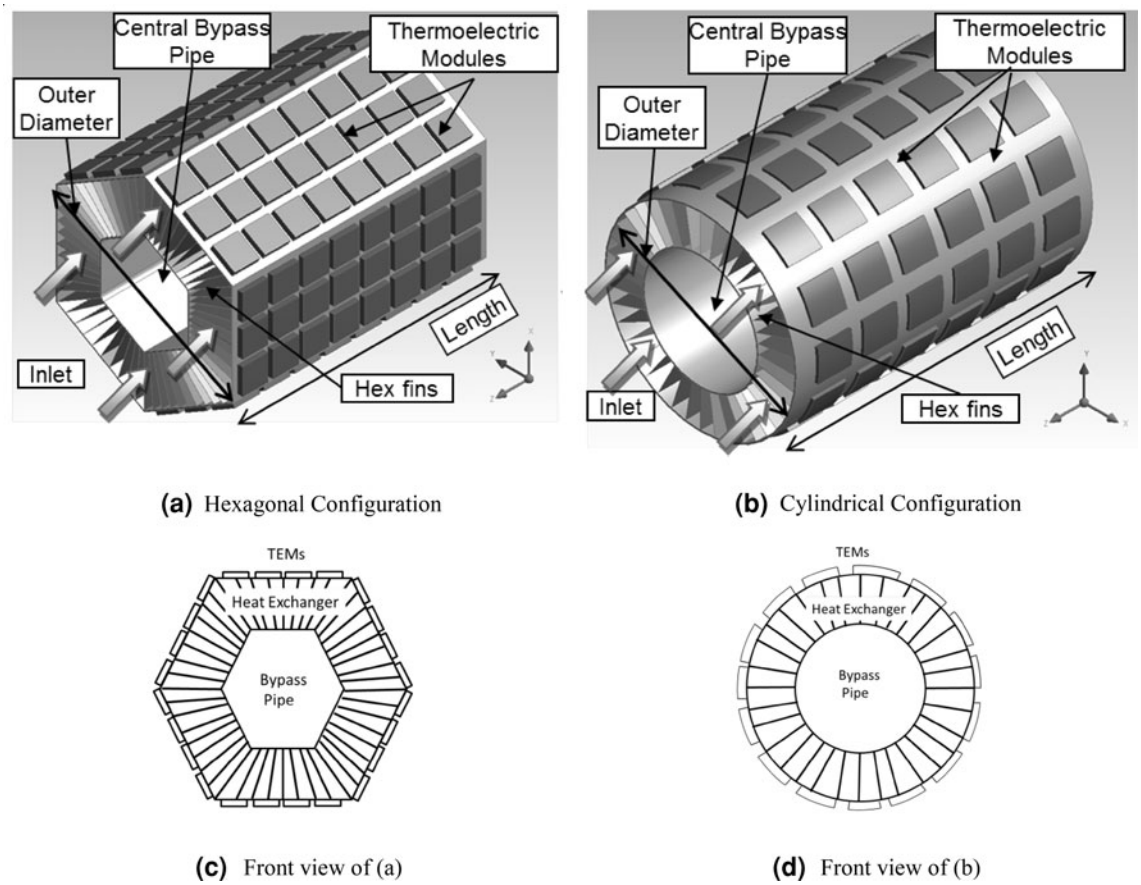


Fig. 2. Circular topologies, showing the arrangement of thermoelectric modules, heat exchanger placement, and exhaust flow direction through the thermoelectric generators.

model. The exhaust gas enters a plenum which distributes the gas axially into several channels shown as red dotted lines (Fig. 1d). In this model, the TEMs are stacked vertically as racks in the transverse direction with respect to the flow path. The hot side of the TEMs is directly exposed to the hot exhaust gas channels with integrated heat exchangers. The coolant supply runs from bottom to top, as indicated by blue arrows.

### Circular Topology

Topologies having circular geometry are also considered as test models in this study. Two types of circular configuration: (i) regular hexagon and (ii) cylinder are shown in Fig. 2. These models are similar to the longitudinal model except the cross-section is hexagonal or cylindrical. The circular topologies have the TEMs mounted on the outer surface of the duct, as shown in Fig. 2a and b for hexagonal and cylindrical configurations, respectively. The annular region is integrated with plate fins running along the length of the generator. The inner duct acts like a central bypass pipe to offset high-temperature or back-pressure effects.

## TEG MODELING

The tool developed in part I of this study is adapted to model the topologies described in the previous section. The key is to correctly identify the control volumes for each topology and model the effective heat exchanger and resistive branches as done previously. The details of the longitudinal model were extensively discussed in part I.[1] In this report, parameters specific to the heat exchanger such as fin thickness, fin spacing, or the number of fins are investigated/optimized, and then the arrangement and geometry (width, height, and length) of the TEMs are varied within prescribed bounds to compute outputs such as the electrical power and associated pressure drops.

For the transverse model, a repetitive element is chosen as a representative control volume, which could effectively model the entire TEG as shown in Fig. 1d. The thermal resistance methodology is applied to this control volume to solve for the electrical and thermal fluxes in the transverse TEG domain. Then, the outputs obtained are scaled to twice the number of TE racks along the transverse-direction TEG width to obtain a complete solution

**Table I. User inputs for parametric analysis**

| Parameter | Value | Unit |
|---|---|---|
| Geometry | | |
| Thermoelectric generator volume | 0.003592 | $m^3$ |
| Exhaust inlet and outlet pipe diameter | 0.0635 | m |
| Dimensions for rectangular topology (length, height, width) | (0.01–2.0, 0.01–0.35, 0.01–1.2) | (m, m, m) |
| Dimensions for circular topology (outer diameter, inner diameter) | (0.05–0.20, 0.01–0.04) | (m, m) |
| Fins (copper) (thickness $t_f$, spacing $s_f$) | (1–8, 1–8) | (mm, mm) |
| Thermal conductivity | 401 | $W\ m^{-1}\ K^{-1}$ |
| Thermoelectric module | | |
| Skutterudite | | |
| Module (cross-section, height) | (0.0508 × 0.0508, 0.007) | ($m^2$, m) |
| TEC ($N_{TEC}$, cross-section, height) | (32, 0.004 × 0.004, 0.004) | (–, $m^2$, m) |
| $\varepsilon_{Module}$ (ceramic) | 0.55 | (–) |
| Thermoelectric material | $Ba_{0.08}La_{0.05}Yb_{0.04}Co_4Sb_{12}$ ($n$-type)[7] | (–) |
| | $DD_{0.76}Fe_{3.4}Ni_{0.6}Sb_{12}$ ($p$-type)[6] | (–) |
| Bismuth telluride | | |
| Module (cross-section, height) | (0.04013 × 0.04013, 0.004) | ($m^2$, m) |
| TEC ($N_{TEC}$, cross-section, height) | (127, 0.002 × 0.002, 0.002) | (–, $m^2$, m) |
| $\varepsilon_{Module}$ | 0.55 | (–) |
| Thermoelectric material | $Bi_2Te_3$[8] | |

for the TEG as a function of path length along the TEG. For circular topologies, the control volume is taken as an annular duct with axial length running along the exhaust flow direction. The average diameter of the cross-section is used to determine the pitch of the heat exchanger system. A method similar to that described previously is applied to compute equivalent thermal resistance networks for these topologies.

## Hybrid Configuration

As mentioned in the "Introduction," the thermoelectric modules used should be selected according to the temperatures along the TEG. The details of modules based on skutterudite and bismuth telluride are presented in Table I. In this work, modules based on bismuth telluride[8] are considered at the rear section of the TEG, as they perform better than skutterudites at lower hot-side temperatures. Figure 3 shows the $ZT$ values of thermoelectric couples (TECs) based on skutterudite and bismuth telluride. The $ZT$ calculations for a TEC were discussed in part I of this study.[1] To maximize $ZT$ performance and protect the bismuth telluride-based modules from damage, the cutoff temperature for the transition is set at 280°C.

## Model Inputs

The parametric study includes a number of input parameters that are varied to optimize the efficiency or power output. Modeling details can be found in part I.[1] The additional parameters studied here are presented in Table I. The ranges of the parameters for different topologies were calculated based on a constant TEG volume of 3.6 L. Properties of the TEMs were provided by Marlow Industries. The inlet conditions are the same as those used for the baseline model study in part I. The average inlet conditions were chosen as $\dot{m}_{in}$ = 35 g/s and $T_{in}$ = 550°C.

## Model Verification

Grid independence analysis was carried out for all the topologies to ensure that the solution set was independent of the domain discretization. Figure 4 shows the dependence of electrical power and relative error on grid size for the hexagonal model with outer diameter ($d_o$) = 0.105 m, inner diameter ($d_i$) = 0.04 m, fin thickness ($t_f$) = 0.002 m, and number of fins ($N_f$) = 60 at average inlet conditions. The numerical code was run for various grid sizes ranging from as coarse as 2 to as fine as 128 elements along the flow direction. Grid independence analysis was carried out to compute reasonable grid sizes for various domain sizes for each topology.

The code was also verified to ensure energy conservation. The enthalpy influx rate $\dot{H}_{in}$ was calculated by multiplying the dry air enthalpy at 550°C by a mass flow rate of 35 g/s ($T_{ref}$ = 100°C). Similarly, the enthalpy outflow $\dot{H}_{out}$ was calculated under the same condition using exit temperatures. The enthalpy change $\Delta\{H = \dot{H}_{in} - \dot{H}_{out}$ is the energy transferred by the gas to the generator. $\dot{Q}_{coolant}$ is the rate at which energy is rejected due to conduction from the module cold side and radiative effects. $\dot{Q}_{trf}$ is the sum of the generated electrical power ($P_{el}$) and the heat rejection ($\dot{Q}_{coolant}$). The energy imbalance ($|Err|$) is computed from the difference of $\dot{Q}_{trf}$ and $\Delta\dot{H}$. The relative error (%) for the hexagonal model was found to be 0.041%. However, the maximum relative error for other models for different configurations was found to be less than 0.05%, as presented in Table II.

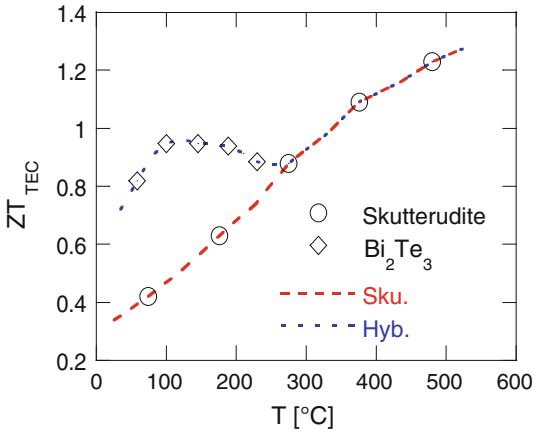


Fig. 3. *ZT* for thermoelectric couples (TECs) based on skutterudite and $Bi_2Te_3$.[6–8]

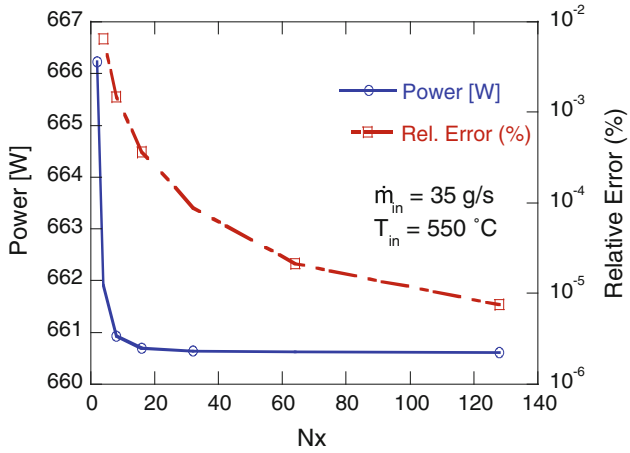


Fig. 4. Grid independence study for the hexagonal model at average inlet conditions.

**Table II. Global energy balances for hexagonal topology**

| Model | $\dot{H}_{in}$ (W) | $\dot{H}_{out}$ (W) | $\Delta\dot{H}$ (W) | $\dot{P}_{el}$ (W) | $\dot{Q}_{coolant}$ (W) | $\dot{Q}_{trf}$ (W) | \|Err\| (W) | Err (%) |
|---|---|---|---|---|---|---|---|---|
| Hexagonal | 29,669.5 | 19,792.5 | 9877 | 660.6 | 9220.4 | 9881 | 0.0004 | 0.041 |

## RESULTS

The topologies were run for various parameters such as heat exchanger characteristics (number of fins and fin thickness), TEM arrangement, and geometry. Firstly, the impact of the parameters on the longitudinal model is described in detail. Then, the performance analyses of other topologies are presented.

### Longitudinal Model

Comprehensive analysis of GM's baseline model was presented in part I of this study.[1] The effect of varying inlet conditions on the power generation and associated pressure drop is presented for a fixed geometry and heat exchanger topology. In this section, the influence of parameters such as the heat exchanger design (number of fins and fin thickness), geometry, and TEM configuration on the baseline model is presented.

#### *Effect of Heat Exchanger Design*

Figure 5a presents the electrical power generation for different fin configurations for average inlet conditions of $\dot{m}_{in}$ = 35 g/s and $T_{in}$ = 550°C for a TEG comprised exclusively of skutterudite modules. This figure shows that the power output increases with the number of fins of varying thickness ranging from 2 mm to 8 mm. It is observed that, for a given number of fins, thinner fins incur comparatively smaller pressure drops as shown in Fig. 5b. Both electric power output and pressure drop values increase with the number of fins. Larger numbers of fins will result in higher cost and weight of the thermoelectric generator, and so an optimized trade-off needs to be evaluated. Configurations with optimized number of fins and thickness can put out 600 W to 700 W of electricity with pressure drops within the allowed back-pressure limits.

#### *Arrangement of TEMs*

Figure 6 shows the benefit of using the hybrid arrangement of modules on the power output for varying inlet conditions. It is exhibited that, for a given surface area and inlet conditions, more electrical power can be generated by the use of hybrid configurations (shown by dashed lines) than using the skutterudites alone (solid lines). The blue lines represent TEGs with the basic heat exchanger configuration with $t_f$ = 3.3 mm and $N_f$ = 22, whereas the red lines (Hex Opt.) are for the optimized heat exchanger configuration with $t_f$ = 2 mm and $N_f$ = 55. However, there is a large mismatch in internal electrical resistances of the bismuth telluride and skutterudite modules. Hence, it becomes quite difficult to match the external electrical load, which makes practical application of this TEM arrangement design very difficult.

Table III presents the improvement in system performance for pure skutterudite and hybrid configurations at average inlet conditions. TEGs with optimized heat exchanger configuration and hybrid arrangement of TEMs show a power conversion rate of 5.35% of incident energy, as compared with 3.33% for the baseline configuration (Sku.). The incident flux was calculated from the air enthalpy property

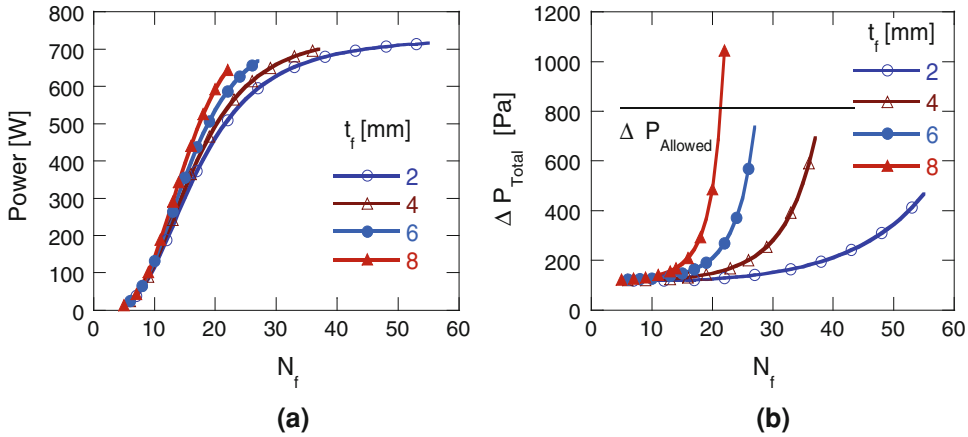


Fig. 5. Power output (a) and pressure drop (b) versus fin thickness ($t_f$) and number of fins ($N_f$) at average inlet conditions for the longitudinal model (width = 0.224 m, height = 0.038 m, length = 0.413 m).

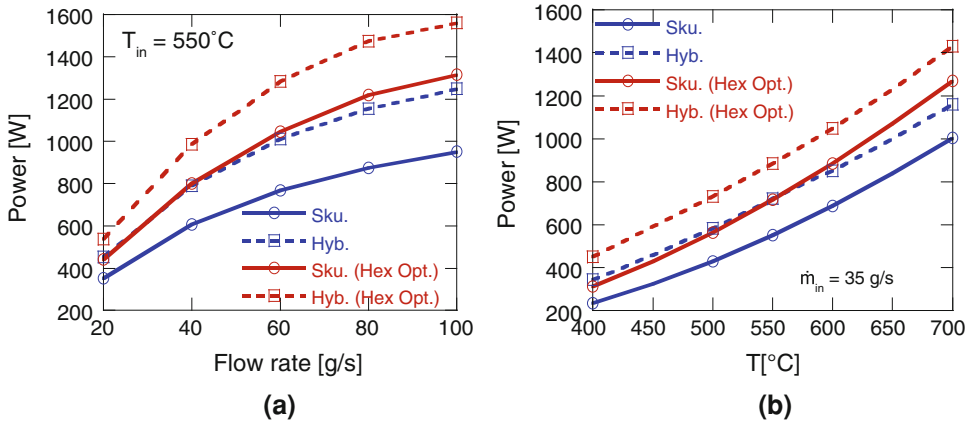


Fig. 6. Electrical power output (a) at various inlet conditions for pure skutterudite (Sku.) and hybrid (Hyb.) arrangements of TEMs for a longitudinal model. Results for similar configurations with optimized heat exchangers are denoted by (Hex. Opt) and are presented in (b).

**Table III. System efficiency for longitudinal model at average inlet conditions**

| Configuration | $\eta_{TE}$ (%) | $\eta_{Heat\ Ex.}$ (%) | $\eta_{System}$ (%) | $\dot{P}_{el}$ (W) |
|---|---|---|---|---|
| Sku. | 5.37 | 52.21 | 3.33 | 552 |
| Sku. (Hex Opt.) | 6.22 | 59.20 | 4.35 | 716 |
| Hyb. | 6.32 | 57.23 | 4.32 | 722 |
| Hyb. (Hex. Opt.) | 6.98 | 64.53 | 5.35 | 886 |

with $T_{ref}$ = 100°C. Optimization of the heat exchanger enhances the heat transfer through the TEMs by 7% to 8% and hence increases the electrical power generation efficiency.

### *TEG Geometry Optimization*

The geometry of the model was varied, keeping the total volume constant at 3.6 L, which was the volume of the baseline design.[1] The length, width, and height of the generator were varied within constraints defined for automobiles (Table I) at average inlet conditions. The configurations were fitted with optimized heat exchanger configurations. Topologies with pressure drop exceeding 812 Pa were disregarded. Figure 7 represents a three-dimensional (3-D) plot of electrical power output for the skutterudite-only arrangements. It is observed that wider and flatter (minimum height) generators produce the maximum possible electrical power.

Another analysis was performed, keeping the height the same as in the baseline design (38 mm) but changing the aspect ratio (=width/length) to accommodate 50 skutterudite modules on the top

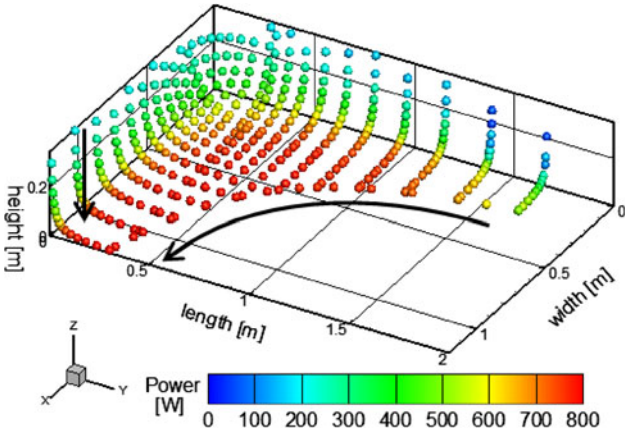


Fig. 7. Three-dimensional plot of electrical power output for longitudinal model with optimized heat exchanger configurations at average inlet conditions.

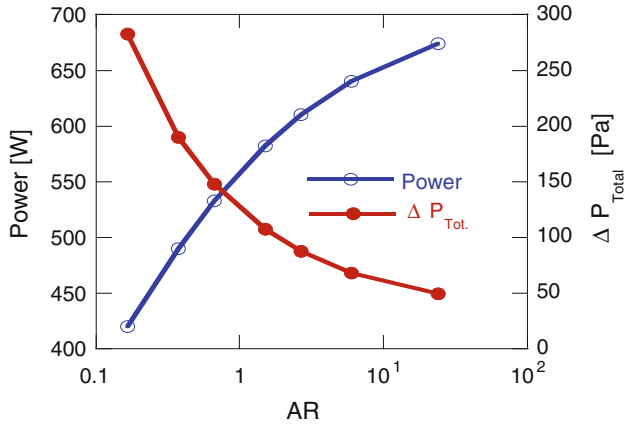


Fig. 8. Power output and pressure drop variation at different aspect ratios (AR = width/length) at fixed TEG height of 38 mm using 50 skutterudite TEMs with fixed heat exchanger specifications ($t_{fin}$ = 3.3 mm, $s_{fin}$ = 6.35 mm) at average inlet conditions.

and bottom surfaces of the generator while keeping the volume constant. Figure 8 shows that the power output is higher for high aspect ratios (wider generators) and associated pressure drops are lower due to shorter path lengths.

The analyses of the longitudinal flow configurations suggest that the heat exchanger configurations play a major role in the electrical output and pressure drops. Use of an optimized number and thickness (or spacing) of fins can help generators produce electrical output in the range of 600 W to 700 W while keeping the back-pressure gain well below 812 Pa for average inlet conditions. Use of hybrid arrangements of thermoelectric modules is an advantage in terms of electrical power generation for a given inlet condition. Wide and flat heat exchangers in a thermoelectric device (with a minimum practical height) help generate the maximum possible electrical power of the order of 800 W. Wider and shorter (in length) generators exhibit much higher electrical power output and significantly lower associated pressure drops for a given number of thermoelectric modules.

## Transverse Model

This section presents analysis of a transverse configuration within a rectangular topology. The parameters of interest for optimization are the hot gas channel width, heat exchanger, and number of TEMs. The number of racks inside the box volume controls the total number of TEMs for a given rectangular shape.

### *Hot Gas Channel Width*

Figure 9 represents the effect of changing the channel width on the power output, number of modules, and pressure drop for a transverse design with optimized heat exchanger configurations. The channel width controls the total number of TE racks inside the TEG volume, hence the number of modules that can be accommodated decreases as the channel width increases as shown on the right axis. Similarly, the power output also decreases with increasing channel width. The curve has a staircase pattern and shows a drop once a thermoelectric module rack is eliminated. There is a sudden drop in power output for very small channel width because the effective heat exchanger area decreases and hence the heat transfer to the modules is inadequate. In addition, the pressure drops are much higher than the allowed limits for lower channel widths; hence it becomes difficult to optimize configurations with lower channel widths, as shown in Fig. 9. As the channel width increases, the number of channels decreases, as does the Reynolds number; hence the pressure drop also decreases.

### *Effect of Geometry*

Several geometric configurations were tested by modifying the aspect ratios of the transverse configurations. The TEG length was fixed as a multiple of the module side; i.e., only one module is placed along the length of the TEG. This was done to ensure that thermoelectric modules face the highest gas temperatures at the hot side. The aspect ratio (width/height) was varied, and its impact was studied. The geometries with an optimized heat exchanger configuration and optimized number of skutterudite modules, and pressure drop within the predefined limit, were considered for full analysis.

Figure 10a shows the electrical power output for varying aspect ratios using three different exhaust gas flow rates. It is found that the power generation does not vary much with the geometry changes due to the fact that the optimized heat exchanger design compensates for the loss in power. This result can be accounted for by the fact that all the thermoelectric modules are subjected to the same hot gas bulk temperature (since the TEG length is one module height). However, there is a significant increase in the electrical power output as the mass flow rates

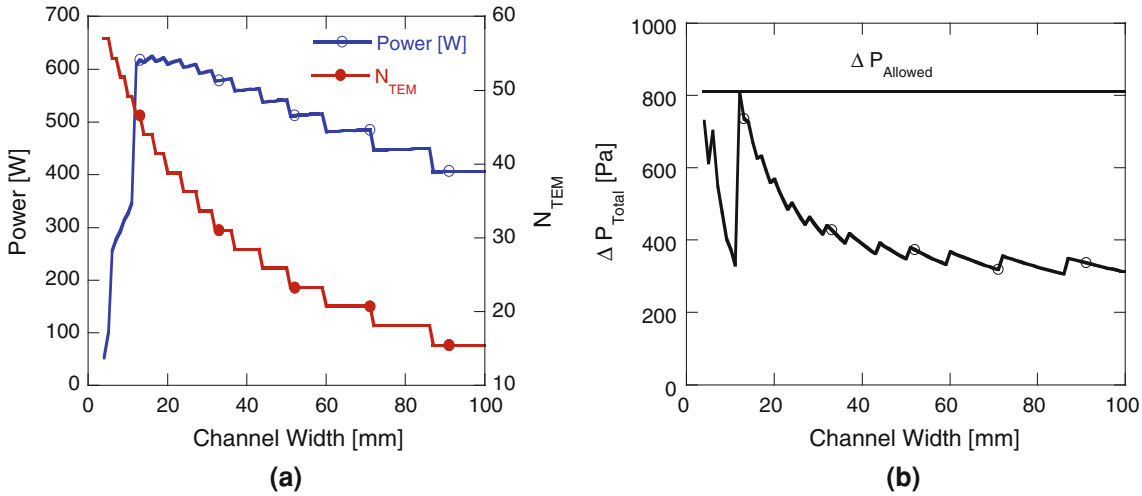


Fig. 9. (a) Left axis: electrical power output versus channel width for transverse model (height: 3.8 cm, width: 22.4 cm, length: 41.3 cm) equipped with optimized heat exchangers. Right axis: required number of skutterudite modules. Associated pressure drop versus channel width is shown in (b).

increase, which was also the case for the longitudinal configuration. The number of TEMs required to achieve the generation rate at various aspect ratios is shown in Fig. 10b. It is found that 50 to 60 is the required range of number of skutterudite modules, regardless of flow rate. The pressure drops for these cases were found to be less than 60% of the allowed back-pressure limit. This could be explained by the fact that the TEG path length is only one module width (5.08 cm), hence pressure drops due to the viscous drag on fins are not significant.

The effect of the number of skutterudite modules was also studied by varying the aspect ratios as shown in Fig. 11a. The number of modules was limited to 20, 40, and 60, and the impact of the total number of modulus on the power output was noted. It is found that the aspect ratio does not have any significant impact on the power output for the transverse configuration. It is important to note that there is not much gain in power output if the number of modules is switched from 40 to 60, which is not the case from 20 to 40 modules. Hence, to obtain a power output in the range of 700 W, 40 skutterudite modules will be sufficient. Adding more modules may lead to a slight increase in electrical power output, but will result in additional TEG cost, which will offset the marginal power gains.

The total pressure drop incurred for different aspect ratios for different numbers of modules is shown in Fig. 11b. To accommodate a higher number of thermoelectric modules inside the rectangular domain at a given aspect ratio (TEG width), the channel width has to be reduced. This increases the fin channel Reynolds number and the pressure drop. Again this supports the fact that use of 40 modules in this case would be quite beneficial as opposed to having a larger number of thermoelectric modules, with their associated cost increase without clear performance benefit.

In summary, for the transverse configuration, the electrical power output is a strong function of the inlet mass flow rate. However, the optimized numbers of modules are independent of the inlet conditions and the aspect ratio. Analysis of the transverse model indicates that 40 skutterudite modules are sufficient to generate a power output of 680 W at the average inlet conditions when the TEG length is equal to one skutterudite module width. A marginal gain in electrical power of 11.7% is observed when the number of modules is increased from 40 to 60. The power output is independent of aspect ratio, since the thermoelectric modules are subjected to the same gas bulk temperature within the TEG length. The associated pressure drops are found to be quite low since the TEG length is restricted to one module width.

## Circular Topology

This section discusses the topologies having radial symmetry. The central bypass pipe is a common feature for these topologies. This protects the thermoelectric modules from overheating, high back-pressure to the engine, and engine overheating. The modeling results for hexagonal and cylindrical configurations are discussed in the following subsections.

## Hexagonal Topology

The cross-section of the regular hexagon is inscribed in a circle of inner ($D_I$) and outer ($D_O$) diameters. The effects of varying these two diameters on the power output and pressure drop were studied with the imposed condition of a constant 3.6 L volume. The bypass pipe space was also counted in the TEG volume. Figure 12a presents the power output for the average inlet conditions with optimized heat exchanger configurations. The

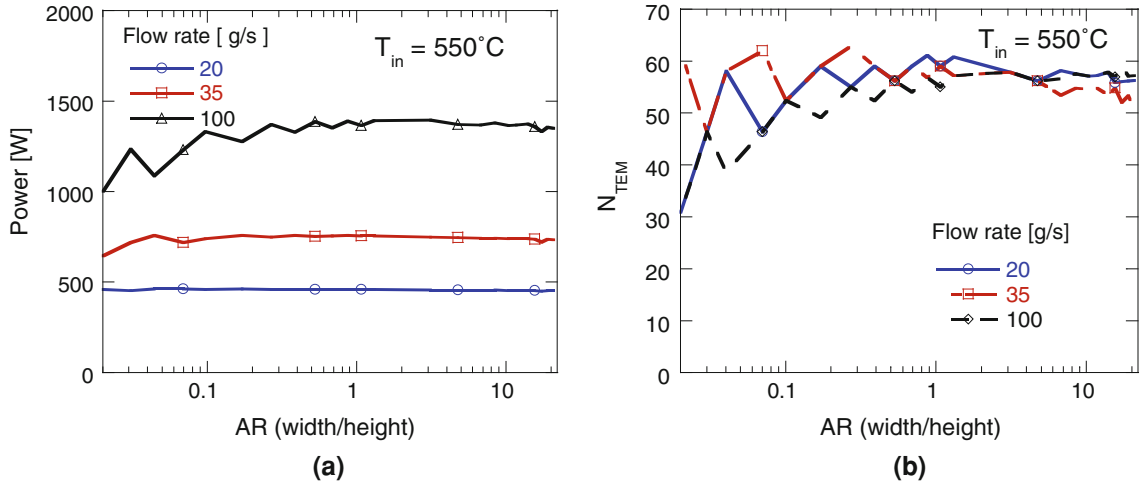


Fig. 10. Electrical power output (a) for various aspect ratios (AR = width/height), keeping the TEG length equal to 5.08 cm (one module width), for optimized heat exchangers. The legend shows the electrical power output at different flow rates. The required number of skutterudite modules is plotted in (b).

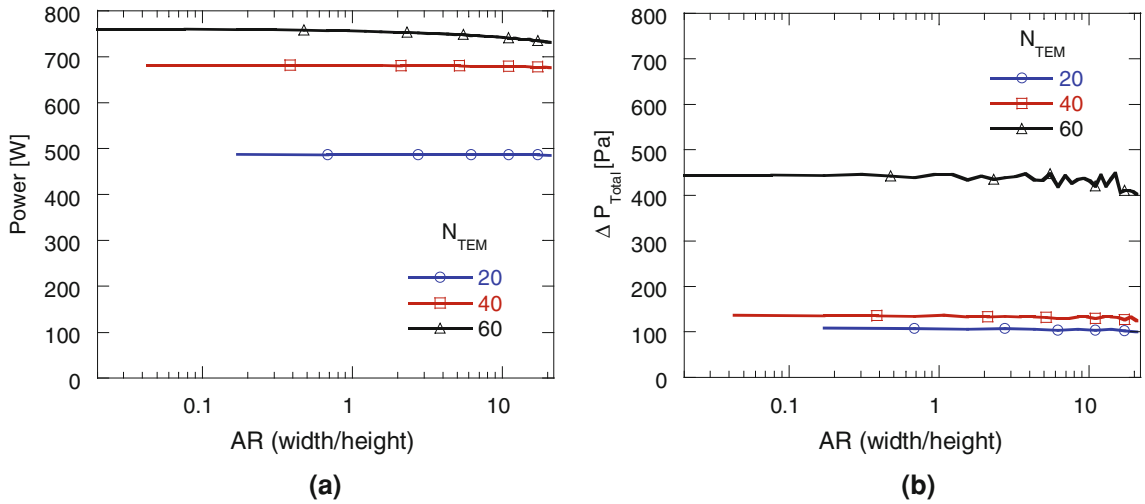


Fig. 11. Optimized power output (a) for various AR (width/height) keeping the length equal to one module side for $\dot{m}_{in}$ = 35 g/s and $T_{in}$ = 550°C. The colored curves show the electrical output for different numbers of skutterudites modules as shown in the legend. Associated pressure drops are also shown in (b).

bypass pipe diameter ($D_I$) was varied from 0.01 m to 0.04 m and $D_O$ from 0.06 m to 0.2 m. It is observed that the power output reaches a maximum of 658 W at $D_O$ of 0.105 m for $D_I$ = 0.04 m. This geometric configuration could accommodate 42 skutterudite modules. The power output is nearly independent of $D_I$ for higher values of $D_O$. However, the power output decreases considerably at higher values of inner diameter. This can be explained by the fact that the effective surface area of the heat exchangers in the annular region decreases. The effective number of skutterudite modules decreases with increasing outer diameter or decreasing generator length due to the fixed volume constraint. The associated pressure drops decrease with increasing outer diameter or decreasing device length as shown in Fig. 12b. The configurations with higher inner diameter lead to smaller annular cross-sections for exhaust gas flow and hence relatively higher pressure drops. The selection of optimized heat exchangers for the outer diameter range of 0.06 m to 0.1 m limits the pressure drop below 812 Pa. This is evident from the zigzag behavior of the pressure curve at lower outer diameters where associated pressure drops are very close to the upper limit.

## Cylindrical Topology

This subsection presents the results for the cylindrical topology. The model is similar to the hexagonal model except that the thermoelectric modules are mounted on the curved outer surface.

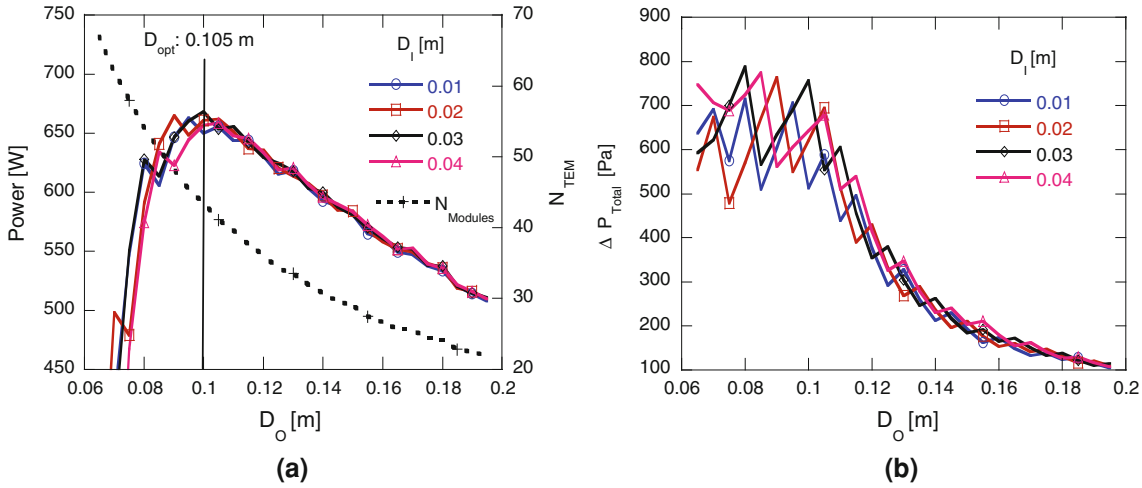


Fig. 12. Power output (a) with varying outer diameter ($D_O$) for different inner diameters ($D_I$) for pure skutterudite configuration at $\dot{m}_{in}$ = 35 g/s and $T_{in}$ = 550°C for optimized heat exchanger configuration. The right *Y*-axis shows the number of modules. Associated pressure drops are shown in (b).

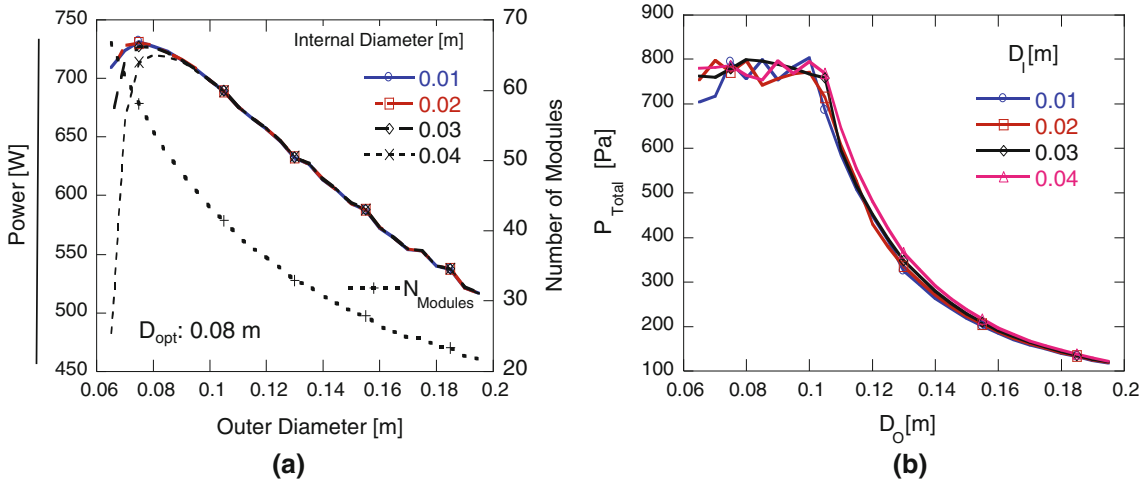


Fig. 13. Power output (a) with varying outer diameter ($D_O$) for different inner diameters ($D_I$) at $\dot{m}_{in}$ = 35 g/s and $T_{in}$ = 550°C for optimized heat exchanger configuration. The right *Y*-axis shows the number of modules. Associated pressure drops are plotted in (b).

However, we note that it will be difficult to achieve good thermal contact on curved surfaces for thermoelectric modules.

The inner and outer diameters of the cylindrical pipes were varied to assess the impact on the generated electrical power and associated pressure drops with optimized heat exchangers. Figure 13a shows that the electrical power output reaches a maximum of 720 W at $D_O$ = 0.08 m and $D_I$ = 0.04 m. It should be noted that, for a given $D_O$ (inscribed circle diameter for hexagon and outer diameter of cylinder), the surface areas of the hexagonal and cylindrical designs are equal and allow an equal number of TEMs to be mounted. However, the comparatively lower cross-sectional area of the cylindrical topology leads to a higher Reynolds number and consequently higher heat transfer rates through the TEMs. Hence, the cylindrical configuration performs better than the hexagonal configuration by 50 W to 60 W of electrical power.

The hexagonal and cylindrical topologies were also studied to compare pure skutterudite designs and hybrid arrangements of TEM modules. It should be noted that optimized outer diameters were selected for the cylindrical and hexagonal cross-sections as taken from the analysis at average inlet conditions. These arrangements were studied for varying inlet conditions including mass flow rate and inlet exhaust gas temperatures as shown in Fig. 14. The trends in power generation are similar to the baseline longitudinal configuration. In addition, it is observed that the cylindrical model outperforms the hexagonal model in terms of power generation for varying conditions. A cylindrical

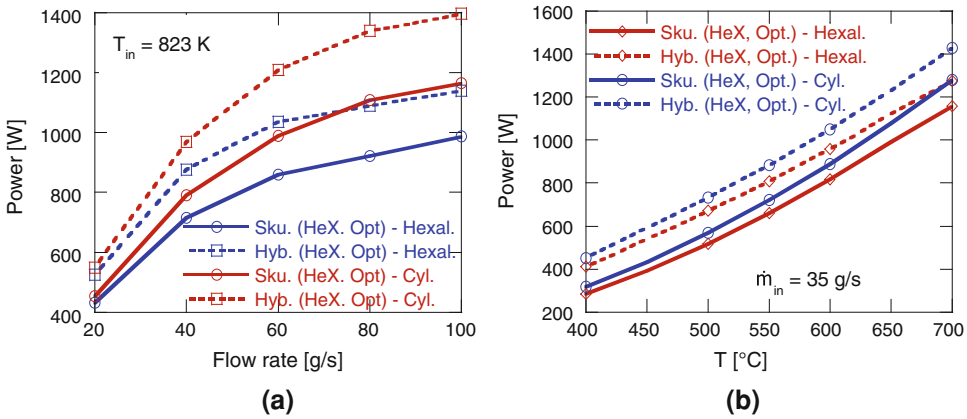


Fig. 14. Power output with varying inlet conditions for hexagonal (blue) with $D_O$ = 0.105 m and $D_I$ = 0.04 m and cylindrical (red) with $D_O$ = 0.08 m and $D_I$ = 0.04 m models for pure skutterudite (solid line) and hybrid (dashed line) arrangements with optimized heat exchanger configuration.

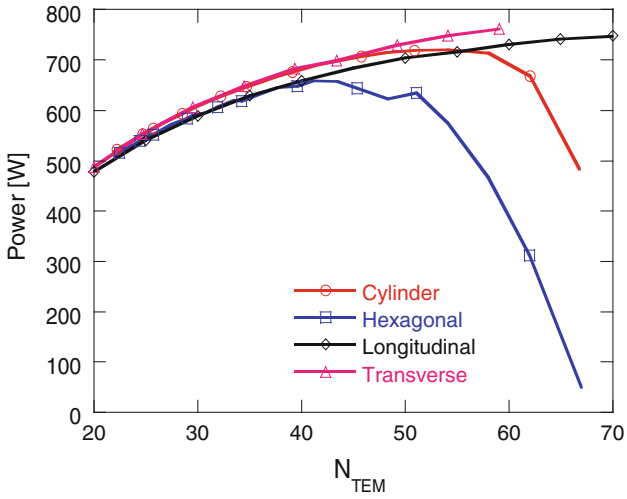


Fig. 15. Effect of the number of skutterudite modules on the electrical power output for various TEG designs.

model with higher optimized $D_O$ can accommodate a comparatively higher number of TEMs and hence generates higher electrical power.

In summary, for the circular topologies, a relatively shorter outer diameter exhibits higher electrical power output and higher pressure drops (larger TEG length). The number of TEMs that can be accommodated decreases with increasing diameter or decreasing length. An optimum $D_O$ exists for maximum electric power output for the hexagonal model (0.105 m with 658 W) and cylindrical model (0.08 m with 720 W) for $D_I$ of 0.04 m. The electrical power output is nearly independent of $D_I$ with $D_O > 0.09$ m. However, the power output decreases considerably if $D_I$ is 50% of $D_O$ or above. Cylindrical topologies perform much better than their hexagonal counterparts for a given number of TEMs or $D_O$. In addition, hybrid arrangements guarantee higher electrical power output for a given heat exchanger configuration and inlet conditions.

## Topology Comparison

In Fig. 15, the four topologies are compared for varying numbers of skutterudite modules, assuming gas inlet conditions of $\dot{m}_{in}$ = 35 g/s and $T_{in}$ = 550°C. The model results are for optimized geometry and with optimized heat exchanger configuration. It is evident from Fig. 15 that all four models show an almost linear increase in electric power generation up to 40 skutterudite modules. Transverse flow configurations fail to accommodate 60 modules or more given the volume constraints. Topologies having circular flow configuration cannot accommodate larger numbers of modules as their length decreases. However, these models with longer TEG flow lengths lead to considerable pressure drops, making them undesirable. Overall, the transverse configuration is superior, but differences between it and the circular topology are very small up to a configuration which can accommodate at least 50 skutterudite modules; above this point the transverse configuration shows marginally superior performance.

Table IV presents the energy distribution and device efficiencies for a 50-skutterudite-module design for the different topologies. The transverse model shows maximum electrical power output as compared with other TEG topologies with best possible configurations for a given volume. Enthalpy rates at inlet and outlet ports were calculated using dry air properties with a reference temperature of 100°C. Rectangular topologies exhibit a linear increase in electric power generation up to 40 skutterudite modules except that circular topologies with higher number of modules have considerable pressure drops, making them inefficient (to accommodate 65 modules, the length should be >1 m). Transverse flow configurations fail to deliver after 60 TEMs, since it becomes difficult to accommodate a higher number of thermoelectric modules in the given volume.

**Table IV. Comparison of four models for 50 skutterudite modules**

| Model | $\dot{P}_{el}$ (%) | $\dot{Q}_{Rad}$ (%) | $\dot{Q}_{coolant}$ (%) | $\dot{Q}_{out}$ (%) | $\eta_{Hex}$ (%) | $\eta_{TE}$ (%) | $\dot{P}_{el}$ (W) | $\Delta P_{Total}$ (Pa) |
|---|---|---|---|---|---|---|---|---|
| Longitudinal | 4.26 | 2.44 | 61.3 | 32.0 | 68.0 | 6.4 | 698.3 | 268.5 |
| Transverse | 4.40 | 1.69 | 61.1 | 32.9 | 67.1 | 6.7 | 729.8 | 182.7 |
| Hexagonal | 3.81 | 1.89 | 57.9 | 36.4 | 63.6 | 6.2 | 634.4 | 775.3 |
| Cylindrical | 4.33 | 1.77 | 61.4 | 32.5 | 67.5 | 6.6 | 718.9 | 753.6 |

## CONCLUSIONS

The numerical model described in part I of this study is adapted to an array of topologies to analyze their performance as thermoelectric generators for waste heat recovery in automotive exhaust systems. Parametric evaluation of a longitudinal configuration has been discussed in detail, and hence optimization of the baseline model with respect to heat exchanger design, overall geometry, and thermoelectric module configuration is summarized. This tool is further utilized to analyze topologies with different shapes and TEM arrangements to maximize electrical power generation for given TEG volume of 3.6 L.

Results from the parametric evaluation of the longitudinal model indicate that TEG performance improves for configurations that have minimum TEG height and maximum TEG width. This result stems from the fact that the skutterudites perform best at high temperature. Hence, the maximum power is obtained in a parallel flow arrangement in which many skutterudite TECs are exposed to the hottest gas. The hybrid arrangement outperforms the design using only skutterudites. Including fins to augment the heat transfer is highly beneficial and improves the power output by 23% to 31% for longitudinal configurations. Optimal arrangements tend to lie near engine back-pressure performance limits.

All topologies behave somewhat similarly at lower numbers of TEMs in terms of electrical generation. However, the performance of the hexagonal and cylindrical topologies suffers when the number of TEMs exceeds 40 owing to large pressure drops. The cylindrical design outperforms the hexagonal design in terms of power generation for given volume and number of TEMs. Overall, the transverse design is found to be an improvement over traditional, longitudinal designs. A transverse TEG with a single module length is found to be the most favorable design among all the designs studied, with the highest electrical power generation and lower pressure drops.

## ACKNOWLEDGEMENTS

The research presented was made possible with the financial support of the National Science Foundation (NSF) and US Department of Energy (DOE) (CBET-1048616). We would like to thank Michael Reynolds of GM R&D for helpful discussions and assistance with acquiring the vehicle engine and exhaust data used in this study.

## REFERENCES

1. S. Kumar, S.D. Heister, X. Xu, J.R. Salvador, and G.P. Meisner, *J. Electron. Mater*. (in press).
2. G.P. Meisner, *Thermoelectrics Application Workshop*, San Diego (2011).
3. G.P. Meisner, *Directions in Engine-Efficiency and Emissions Research* (Detroit: DEER) Conference Presentations, 2011.
4. D.T. Morelli, *Proceedings of 15th International Conference on Thermoelectrics 1996*, pp. 383–386 (1996).
5. D.T. Crane and J.W. LaGrandeur, *J. Electron. Mater.* 39, 2142 (2009).
6. G. Rogl, A. Grytsiv, E. Bauer, P. Rogl, and M. Zehetbauer, *Intermetallics* 18, 57 (2010).
7. X. Tang, Q. Zhang, L. Chen, T. Goto, and T. Hirai, *J. Appl. Phys.* 97, 093712 (2005).
8. X.B. Zhao, X.H. Ji, Y.H. Zhang, T.J. Zhu, J.P. Tu, and X.B. Zhang, *Appl. Phys. Lett.* 86, 062111 (2005).